

## Comissão 3.3 - Manejo e conservação do solo e da água

# MORPHOLOGICAL AND MICROMORPHOLOGICAL CHANGES IN THE STRUCTURE OF A RHODIC HAPLUDOX AS A RESULT OF AGRICULTURAL MANAGEMENT

Laura Fernanda Simões da Silva<sup>(1)\*</sup>, Mara de Andrade Marinho<sup>(1)</sup>, Edson Eiji Matsura<sup>(1)</sup>,  
Miguel Cooper<sup>(2)</sup> and Ricardo Ralisch<sup>(3)</sup>

<sup>(1)</sup> Universidade Estadual de Campinas, Faculdade de Engenharia Agrícola, Campinas, São Paulo, Brasil.

<sup>(2)</sup> Universidade de São Paulo, Escola Superior de Agricultura Luiz de Queiroz, Departamento de Ciência do Solo, Piracicaba, São Paulo, Brasil.

<sup>(3)</sup> Universidade Estadual de Londrina, Centro de Ciências Agrárias, Londrina, Paraná, Brasil.

\* Corresponding author.

E-mail: laurafsimoes@yahoo.com

### ABSTRACT

In evaluation of soil quality for agricultural use, soil structure is one of the most important properties, which is influenced not only by climate, biological activity, and management practices but also by mechanical and physico-chemical forces acting in the soil. The purpose of this study was to evaluate the influence of conventional agricultural management on the structure and microstructure of a Latossolo Vermelho distroférico típico (Rhodic Hapludox) in an experimental area planted to maize. Soil morphology was described using the crop profile method by identifying the distinct structural volumes called Morphologically Homogeneous Units (MHUs). For comparison, we also described a profile in an adjacent area without agricultural use and under natural regrowth referred to as Memory. We took undisturbed samples from the main MHUs so as to form thin sections and blocks of soil for micromorphological and micromorphometrical analyses. Results from the application of the crop profile method showed the occurrence of the following structural types: loose (L), fragmented (F) and continuous (C) in both profiles analyzed. In the Memory soil profile, the fragmented structures were classified as  $F_{pt\mu\Delta+tf}$  and  $F_{mt\Delta\mu}$ , whose micromorphology shows an enaulic-porphyric (porous) relative distribution with a great deal of biological activity as indicated by the presence of vughs and channels. Lower down, from 0.20 to 0.35 m, there was a continuous soil volume (sub-type  $C_{\Delta\mu}$ ), with a subangular block microstructure and an enaulic-porphyric relative distribution, though in this case more compact and with aggregate

Received for publication on February 7, 2014 and approved on October 10, 2014.

DOI: 10.1590/01000683rbc20150045

coalescence and less biological activity. The micromorphometrical study of the soil of the Memory Plot showed the predominance of complex pores in NAM (15.03 %), Fmt $\Delta\mu$  (11.72 %), and Fpt $\mu\Delta$ +tf (7.73 %), and rounded pores in C $\Delta\mu$  (8.21 %). In the soil under conventional agricultural management, we observed fragmented structures similar to the Memory Plot from 0.02 to 0.20 m, followed by a volume with a compact continuous structure (C $\Delta\mu$ ), without visible porosity and with few roots. In the MHUs under conventional management, reduction in the packing pores (40 %) was observed, mainly in the continuous units (C). The microstructure had well-defined blocks, with the occurrence of planar pores and less evidence of biological activity. In conclusion, the morphological and micromorphological analyses of the soil profiles studied offered complementary information regarding soil structural quality, especially concerning the changes in pore types as result of mechanical stress undergone by the soil.

**Keywords:** crop profile method, soil structure, image analysis, conventional system.

## RESUMO: ALTERAÇÕES MORFOLÓGICAS E MICROMORFOLÓGICAS NA ESTRUTURA DE UM LATOSSOLO VERMELHO DISTROFÉRRICO TÍPICO DECORRENTES DO MANEJO AGRÍCOLA

*Na avaliação da qualidade do solo para uso agrícola, a estrutura é um dos seus atributos mais importantes, sendo não somente influenciada pelo clima, pela atividade biológica e pelas práticas de manejo, como também por forças de natureza mecânica e físico-químicas atuantes no solo. O objetivo deste trabalho foi avaliar a influência do manejo agrícola convencional na estrutura e microestrutura de um Latossolo Vermelho distroférico típico de área experimental cultivada com milho. A morfologia do solo foi descrita conforme o método do perfil cultural, identificando-se as diferentes Unidades Morfológicamente Homogêneas (UMHs). Para fins de comparação, também foi descrito um perfil em área sem uso agrícola e sob revegetação natural referida por parcela Memória. Foram extraídas amostras indeformadas das principais UMHs visando a confecção de lâminas delgadas e blocos de solo destinados às análises micromorfológicas e micromorfométricas. Os resultados revelaram a ocorrência de estruturas dos tipos livre (L), fragmentada (F) e contínua (C) em ambos perfis avaliados. No perfil da parcela Memória, as estruturas fragmentadas são as dos subtipos Fpt $\mu\Delta$ +tf e Fmt $\Delta\mu$ , cuja micromorfologia mostrou uma distribuição relativa enáulica-porfírica (porosa), com grande atividade biológica evidenciada pela presença de cavidades e canais. Mais abaixo, entre 0,20 e 0,35 m, o volume de solo é contínuo do subtipo C $\Delta\mu$ , apresentando microestrutura em blocos subangulares e matriz com distribuição relativa enáulica-porfírica, porém mais compacta e com coalescência de agregados e menor incidência de atividade biológica. O estudo micromorfométrico do solo da parcela Memória revelou predomínio de poros complexos nas unidades NAM (15,03 %), Fmt $\Delta\mu$  (11,72 %) e Fpt $\mu\Delta$ +tf (7,73 %) e de poros arredondados na unidade C $\Delta\mu$  (8,21 %). No solo sob manejo agrícola, observaram-se estruturas fragmentadas similares às da parcela Memória entre 0,02 e 0,20 m seguidas de um volume contínua compacta (C $\Delta\mu$ ), sem porosidade visível a olho nu e com pouquíssimas raízes. Nas UMHs sob manejo convencional, observou-se redução da porosidade de empilhamento (40 %), principalmente nas unidades contínuas (C), com surgimento de formas fissuradas e menor evidência de atividade biológica. Concluindo, as análises morfológicas e micromorfológica dos perfis de solo estudados forneceram informações complementares acerca da qualidade estrutural do solo, em especial quanto às alterações dos tipos de poros decorrentes de estresse mecânico sofrido pelo solo.*

*Palavras-chave:* método perfil cultural, estrutura do solo, análise de imagens, sistema convencional.

## INTRODUCTION

Most studies for the purpose of evaluating soil quality for crop production refer to the effects of characterization and quantification of cultivation and management practices on soil morphological, physical, chemical, and biological properties (Doran, 1987; Bertol et al., 2004; Marques et al., 2010).

However, according to Drees et al. (1994), changes resulting from management on soil properties are

largely consequences of changes undergone by the soil structure. In the case of conventional systems, structural changes arising from intensive mechanization, such as compaction and accelerated soil erosion, may lead to significant changes in soil quality (Hakansson et al., 1988), with a negative effect on infiltration and plant water availability (Imhoff et al., 2000), and soil aeration (Xu et al., 1992), also reducing the depth and exploitable volume of the soil by the roots (Weill and Sparovek, 2008). In addition, for Dexter (2004), the reason for

all symptoms of soil physical degradation is related to structure decay. Thus, structural changes in soil quality often lead to serious consequences both in terms of degradation of this essential, finite, and non-renewable resource, and in economic terms, by bringing about reduced yield or increased costs of production.

Soil structure is a characteristic difficult to measure directly, which is why it is commonly assessed by other properties, such as soil density, porosity (Reynolds et al., 2008), available water (Dexter, 2004), infiltration (Thierfelder and Wall, 2010), soil resistance to penetration and limiting water range (Silva et al., 1994), air permeability (Ball and Schjonning, 2002), tensile strength of aggregates (Guimarães et al., 2009), and the S index (Dexter, 2004).

Qualitative characterization of soil structure through morphological studies at the profile scale and pedogenetic horizons is a traditional approach in Pedology for taxonomic classification (Soil Survey Division Staff, 1993). Gautronneau and Manichon (1987) adapted the morphological study of the soil profile in order to consider the effect of agricultural management and introduced the “crop profile” method. According to the authors, the method allows checking agricultural soils for the physical state of anthropogenic horizons as a result of machine traffic and the work of active components of agricultural implements. In Brazil, the crop profile method was used by Dersigny et al. (1990), Tavares Filho et al. (1999), and Fregonezi et al. (2001) for diagnosis of the structural state of the tilled soil in the field.

Although numerous studies have already shown the utility of the crop profile method for interpretation of the effects of management on soil structural quality (Fregonezi et al., 2001; Tavares Filho and Tessier, 2009), there is a demand for knowing the soil structural organization on a more detailed scale, seeking greater understanding of the structural changes observed in the profile scale. In this context, microscopy and image analysis techniques, which comprise soil micromorphology studies, constitute important tools for direct analysis of the structure by allowing observation of soil constituents, their conformation, arrangement and distribution, and characterization and quantification of types of pores (Castro et al., 2003).

An example of the application of micromorphology in soil structural assessment studies related to agricultural management is the work of Curmi et al. (1994), who studied structure degradation in Latossolos (Oxisols) subjected to cultivation. Using micromorphological techniques, these authors observed that the intra-aggregate pores were not affected by the compression process, but the size and format of the inter-aggregate pores were reduced, and the pores from biological activity (channels) disappeared when subjected to compression

processes. Pagliai et al. (1984) obtained similar results using the same technique in a long-term experiment in vineyards, comparing no-till and conventional management system in a loamy clay Vertisol (Vertic Xerofluvent). These authors clearly observed that the reduction in porosity after tractor traffic was due to a gradual reduction in the size of the elongated pores, following the same trend as total porosity.

In Brazil, the observations made by Souza et al. (2006) from microscopic analysis of thin sections of a Latossolo Vermelho distroférico (Oxisol) planted to citrus also reveal differences in pore space geometry as a result of changes caused by management. Therefore, the purpose of this study was to evaluate the influence of conventional agricultural management on the structure and microstructure of a Rhodic Hapludox in an experimental area planted to maize in the region of Campinas, SP, Brazil.

## MATERIAL AND METHODS

### Description of the study area

We conducted the study in the Experimental Field of the College of Agricultural Engineering, Feagri/Unicamp in Campinas, SP, Brazil in a long-term management trial previously described by Marques et al. (2010). The soil structure assessment described in this study was conducted in the fourth year of that trial, corresponding to the 2006/2007 (summer) crop, with maize grown under a conventional system (CS). The soil is classified according to Embrapa (2013) as a Latossolo Vermelho distroférico típico (Rhodic Hapludox).

For comparison, the same soil was also evaluated in an adjacent area maintained under natural regrowth since 1986, referred to as the Memory Plot. For soil morphological description, we used the Field Soil Description and Sampling Manual (Santos et al., 2013).

### Characterization of the crop profile and identification of the Morphologically Homogeneous Units

To evaluate the soil structural condition, the crop profile method was used. This method was described and adapted for Brazilian soils by Tavares Filho et al. (1999). Characterization of the crop profile was carried out during the maize flowering stage by opening a pit (1.4 m long and 0.6 m deep) perpendicular to the direction of the planting rows and covering two rows of maize. A pit was also opened in the Memory Plot (1.2 m long and 0.5 m deep).

Morphological study of the soil profiles was initiated by observing and separating soil volumes with similar structure, called Morphologically Homogeneous Units (MHUs) by Tamia et al. (1999).

### Collection and preparation of samples for micromorphological analysis

Soil sampling for the micromorphological study was carried out based on identification of the MHUs. An undisturbed soil block with dimensions of  $0.07 \times 0.12 \times 0.06$  m was collected from each representative MHU.

In the laboratory, those undisturbed samples were air dried and impregnated with a solution of polyester resin, styrene monomer, catalyzer, and Tinopal OB (BASF®) fluorescent pigment following the procedures presented by Castro et al. (2003). After impregnation and resin curing, the samples were cut and sanded to a thickness of around 25  $\mu\text{m}$ , appropriate for analysis in an optical microscope.

The thin sections were described using a Zeiss polarizing optical microscope and stereomicroscope under plain polarized light (PPL) and crossed polarized light (XPL). The descriptions followed the criteria and terminology proposed by Bullock et al. (1985) and Stoops (2003). To quantify porosity, the polished soil blocks were illuminated with UV light and photographed with a charged couple device (CCD) of a digital camera (Sony®, Model DFW-X700) coupled to a stereomicroscope.

For each polished block representative of an MHU, several  $12 \times 15$  mm ( $180 \text{ mm}^2$ ) photomicrographs were obtained randomly. We digitized the images with a spatial resolution of  $1024 \times 768$  pixels, each pixel corresponding to an area of  $156.25 \text{ mm}^2$ , a spectral resolution of 256 shades of grey, and a magnification of 10x. For each image, pore segmentation was done by greyscale thresholding.

Subsequently, the images were labelled by the image analysis program Noesis Visilog 5.4. The labeling operation allowed recognition and individualization of the pores in each binary image by means of a connecting factor.

After these steps, the program quantifies the basic variables that refer to the image pore space and the derived variables, defined as discrete entities on the image. Once the basic and derived variables were determined, we classified them according to size classes, shape types, or combinations of both. This procedure was optimized by macros developed in Visual Basic language in Microsoft® Excel developed by Juhász et al. (2007).

Total porosity ( $T_p$ ) was calculated through the sum of the areas of all the pores divided by the total area of the field, in percentage (Hallaire and Cointepas, 1993).

We divided the pores into three groups according to their shape, following Cooper et al. (2010): rounded

(channels and isolated vughs), elongated (planar pores) and complex (packing pores and chambers). Two indexes were used to determine pores shape; the first is referred to as  $I_1$  and calculated by equation 1, used to separate rounded pores from elongated pores. When equal to 1.0,  $I_1$  defines a perfectly circular shape, and when greater than 1.0, it indicates that the pore shape deviates from the circle.

$$I_1 = \frac{P^2}{4\pi A} \quad (1)$$

where  $P$  is the pore perimeter and  $A$  is the pore area occupied.

The second index is referred to as  $I_2$  and calculated according to equation 2. Used as a complement to index  $I_1$ , it allows greater accuracy in separating the shape groups.

$$I_2 = \frac{\frac{1}{m} \sum_i (N_i)_i}{\frac{1}{n} \sum_j (D_F)_j} \quad (2)$$

where  $N_i$  is the number of intercepts of an object in direction  $i$  ( $i = 0^\circ, 45^\circ, 90^\circ, \text{ and } 134^\circ$ ),  $D_F$  the Feret diameter of an object in direction  $j$  ( $j = 0^\circ \text{ and } 90^\circ$ ),  $m$  the number of  $i$  directions, and  $n$  the number of  $j$  directions.

Statistical analyses of the MHUs micromorphometric data were performed and verified for data normality by using the Shapiro-Wilk (1965) test. In addition, analysis of variance was carried out using the F test, and mean comparison by the Duncan test, both at 5 % significance.

## RESULTS AND DISCUSSION

Figure 1 shows the MHUs representation of the Memory Plot profile. From the top to the bottom, the structural types were loose (L), fragmented with variations of the size and internal state of the aggregates ( $F_{pt\mu\Delta+tf}$ ;  $F_{mt\Delta\mu}$ ), and continuous or massive at the profile scale and with variations of the internal state of the aggregates ( $C_{\mu\Delta}$ ). The presence of massive continuous structures demonstrates that although the soil has been kept under fallow for over 25 years, it still exhibits anthropized volumes.

The morphological observations of the profile show that the L structure comprises a thin surface layer with a thickness from  $\pm 0$  to 0.02 m, dark red (10R 2.5/2 moist) and dark-red-grayish (10R 3/4, dry) color, of clayey to very clayey texture, consisting of loose soil, aggregates and clods of varying sizes without any cohesion. The structure was moderate, small to medium in subangular blocks, with a loose consistency, and very friable, plastic, and sticky.

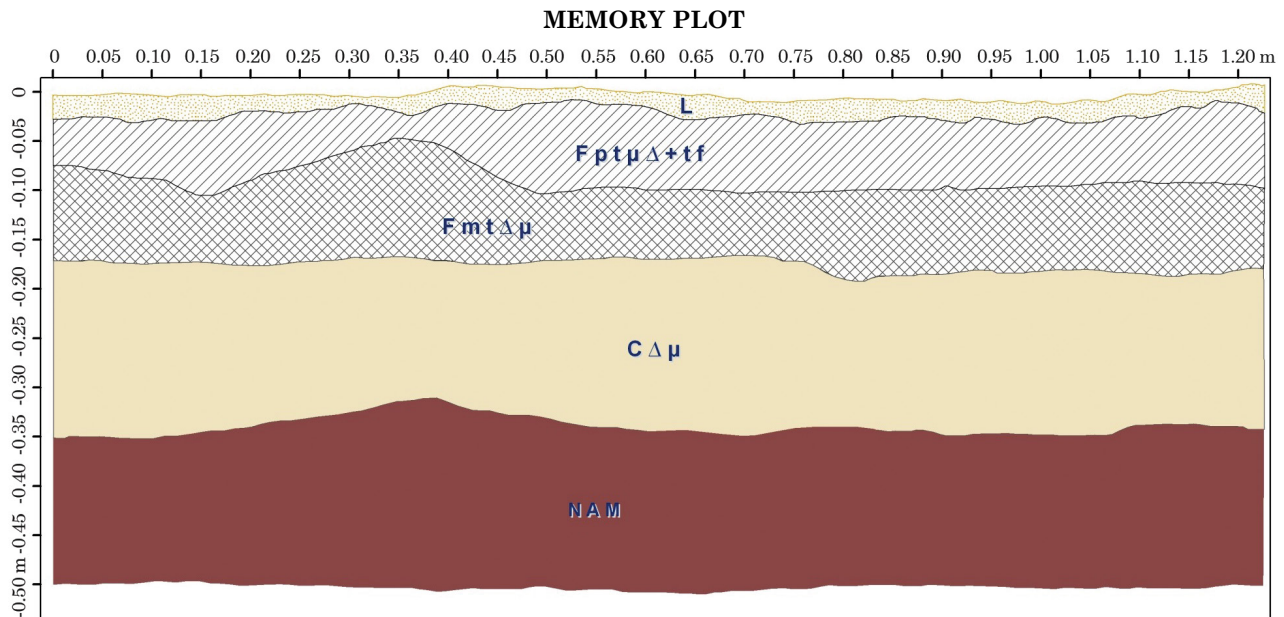


**Figure 1. Schematic representation of the different organizations of the crop profile under the Memory plot.**  
**L:** volume of loose soil, not compact, “powdered”; **F** or **C:** fragmented or continuous volumes of soil; **Δμ** or **μΔ:** compact or porous clods, with very compact aggregates (**Δ**), compact (**Δμ**) and in compaction process (**μΔ**); **pt, mt, gt:** small, medium or large clods; **tf:** fine soil; and **NAM:** not altered by management.

It also had leaf remains, twigs in various stages of decomposition and many non-flattened roots, well branched and in all directions.

Below the L volume, we observed, up to the 0.20 m depth, fragmented structures (F) in small and medium-sized clods (pt and mt), with porous internal structure ( $\mu\Delta$ ) or more compact ( $\Delta\mu$ ) and loose soil (tf) designated by  $Fpt\mu\Delta+tf$  and  $Fmt\Delta\mu$ . A striking feature observed in the F structure is the presence of visible clods at the profile scale due to fragmentation, where the roots had grown preferentially in the spaces between the clods and appeared well branched and in all directions.

The soil volume type  $Fpt\mu\Delta+tf$  was at a depth from  $\pm 0.02$  and 0.10 m, with dark red (10R 2.5/2, moist) and dark red grayish (10R 3/4, dry) color, a clayey to very clayey texture, and a strong structure that was medium-sized, in subangular blocks and a soft, very friable, plastic, and sticky consistency. The internal state of the clods showed characteristics of the compaction process but still maintaining predominant characteristics of the non-compacted state ( $\mu$ ) over the characteristics of the compact state ( $\Delta$ ), indicative of structural resilience. In this case, we associated the recovery of structure to the biological activity evidenced by white grubs, ants, and termites.

The fragmented volume  $Fmt\Delta\mu$ , with medium-sized clods and a compact internal state, occurred at a depth of  $\pm 0.10$ -0.20 m, showing morphological properties (color, texture, consistency, and structure) similar to the previous volume, differentiated only

by the size of the subangular blocks. The porosity among aggregates is large, with the presence of roots with normal development and in all directions, but in smaller quantities compared to the previous volume. With respect to biological activity, we note only the presence of some termites.

From 0.18-0.35 m, a volume of continuous and more compact soil designated as  $C\Delta\mu$  occurred, quite homogeneous, with a massive structure (apedal) aspect at the profile scale; it was not possible to individualize the clods with the naked eye. When material is removed from the profile, it breaks into large angular and subangular blocky aggregates, with a compact internal state ( $\Delta\mu$ ), but still maintaining some characteristics of the non-compact state. The morphological features of color, texture, and consistency are similar to the MHUs previously described ( $Fmt\Delta\mu$  and  $Fpt\mu\Delta+tf$ ). We observed fewer roots and less biological activity compared to the previous MHUs due to the very compact internal state of the clods. However, even in a smaller amount, the roots were branched, not flattened, not twisted, and in all directions.

These findings confirm the results presented by Fregonezi et al. (2001) who observed that fissure porosity, among aggregates, is important for maintaining soil porosity, compensating low intra-aggregate porosity in massive continuous (C) structures, and that porosity in these structures depends more on biological activity, i.e., biological porosity for macropore formation.

Below the 0.35 m depth, the soil was porous and the microaggregate structure was strong, very small and granular, typical of Oxisols, not altered by management (NAM). This MHU had dark red (10R 2.5/2 moist) and dark red grayish (10R 3/4, dry) colors, with very clayey, soft, friable, plastic, and sticky consistency.

Despite the long period out of agricultural use, the soil profile description of the Memory Plot also revealed the occurrence of structures with evidence of compression processes up to the 0.35 m depth. However, signs of recovery of the soil structural quality could be noted, particularly in the fragmented MHUs, where the presence of roots was larger and biological activity was more intense.

Evaluating the organization of the soil volumes found in the crop profile description in CS (Figure 2), there was greater structural variation, evidenced by the higher number of MHUs compared to the Memory Plot profile, reflecting the effect of various management operations under this system. Tavares Filho and Tessier (2009) observed this same trend in the conventional system profile, where they observed a greater MHU subdivision due to anthropization.

At the surface (0.00-0.03 m), there was a loose soil volume (L), non-compacted, porous to the naked eye, consisting of fine soil. The morphological observations of the CS profile revealed that the soil had dark red grayish (10R 3/4, moist) and reddish dark (2.5YR 3/6, dry) colors, a clayey to very clayey

texture, and small, strong, and granular structure, with loose, friable, plastic, and sticky consistency. Roots in large numbers could be observed, which were well branched, not flattened, not twisted, and in all directions. At the same depth, in the plant inter-row region, a Z type volume occurred (laminar structure), denoting a compaction process probably originating from the effect of agricultural machinery traffic in that position.

Just below the L structure, located at a depth of 0.03-0.17 m, several volumes with F-type structures and clods with different internal states were observed (Figure 2). In the plant row, we observed that up to the depth of 0.09 m, the CS crop profile had structure types  $F_{pt\mu\Delta+tf}$  and  $F_{mt\mu\Delta}$ . The MHU type  $F_{ptmD+tf}$  could be found from  $\pm 0.03$  to 0.08 m, with dark red (10R 3/3, moist) and dark red grayish (2.5YR 3/4, dry) colors, a very clayey texture, with strong very small granular and moderate medium subangular blocky structures, and a soft, friable, plastic, and sticky consistency. The  $F_{mt\mu\Delta}$  unit was in  $\pm 0.03$  to 0.09 m area and had color, texture, and consistency similar to the previous unit, differing only in the strong and large angular and subangular blocky aggregates. In the inter-row position, where the traffic was more intense, the MHU was the  $F_{mt\Delta\mu}$  type (Z) at the 0.03-0.14 m depth, in which the aggregates were internally more compressed and with evidence of laminar structure (Z).

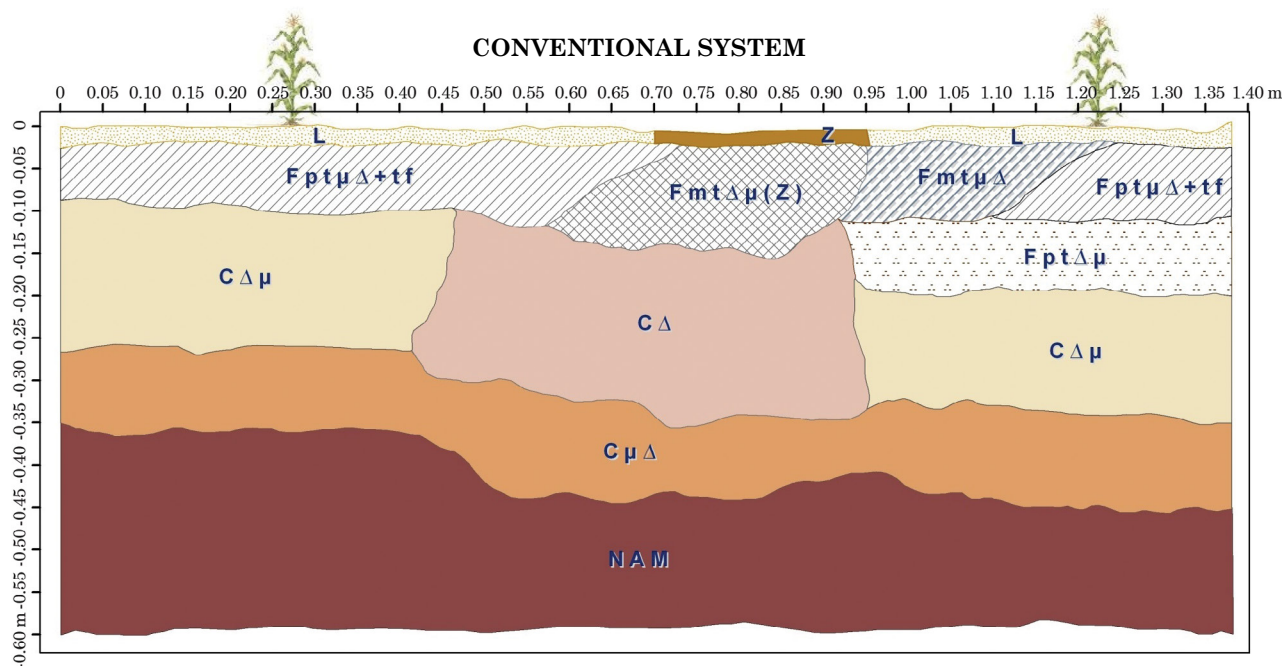


**Figure 2.** Schematic representation of the different organizations of the crop profile under the Conventional System. L: volume of loose soil, not compact, “powdered”; F or C: fragmented or continuous volumes of soil;  $\Delta\mu$  or  $\mu\Delta$ : compact or porous clods, with very compact aggregates ( $\Delta$ ), compact ( $\Delta\mu$ ) and in compaction process ( $\mu\Delta$ ); pt, mt, gt: small, medium or large clods; tf: fine soil; and NAM: not altered by management.

At the 0.07-0.43 m depth, volumes with continuous structure (C) occurred, with variations of the internal condition of the aggregates ranging from  $\Delta\mu$  to  $\mu\Delta$  (Figure 2), constituting quite homogeneous volumes with a massive structure aspect, and it was not possible to individualize the clods visually in the field. The type  $C\Delta\mu$  volume occurred in two places in the profile, from 0.07-0.25 m and from 0.17-0.33 m. These volumes showed morphological characteristics of a dark red (10R 3/3, moist) color, a clayey to very clayey texture, strong and large angular blocks, and friable, plastic, and sticky consistency.

Between these two volumes with  $C\Delta\mu$  structure, there was a type  $C\Delta$  volume with morphological properties similar to the MHUs described above, differing only in the smaller number of roots. Below that, a volume of type  $C\mu\Delta$  located between the depths of 0.24 and 0.43 m, had morphological properties of color, texture, consistency, and structure similar to the  $C\Delta$  MHU described above (Figure 2).

The soil C volumes in the crop profile in CS had fewer roots and less biological activity in relation to type F (fragmented) MHUs. This was expected since the internal state of clods in the massive C volumes is very compact, leading to porosity that is practically nonexistent and restriction of root growth.

At the 0.37-0.57 m depth, the soil was porous and had a microaggregate structure ( $C\mu$ ) similar to the NAM (not altered by management) volumes of the Memory Plot, reflecting natural soil conditions which occur in forest soils, where the structures throughout the profile do not change due to agricultural use (Tavares Filho et al. 1999).

The description of the main soil micromorphological characteristics representative of the different MHUs of the Memory Plot and CS plots are shown in tables 1 and 2, respectively.

The NAM unit of the Memory Plot (Table 1) had a predominantly porphyric-enaulic relative distribution (Figure 3a), with some areas that were purely porphyric and others enaulic. The porphyric-enaulic area had a complex (mixed) microstructure composed of microgranular aggregates with well to moderately developed pedality, partially accommodated, as well as subangular blocky aggregates with moderately developed pedality, partially accommodated. The dominant porosity of this microstructure was compound packing pores (50 %), followed by rounded and policoncave vughs (35 %), planar pores (10 %), and channels (5 %). At the profile scale, the NAM soil unit was porous, with a strong and small granular structure (microaggregates), very similar to the microstructure observed in the thin section.

In the NAM unit, biological activity was evidenced by the widespread presence of rounded vughs and channels with continuous and/or discontinuous loose infillings, which occupied approximately 30 %

of the thin section, corroborating the observations at the profile scale, where biological activity was evidenced by the presence of white grubs, ants, and termites.

Above the NAM unit, the  $C\Delta\mu$  unit had a porphyric relative distribution formed by a complex microstructure made up of subangular blocky aggregates with a moderately developed pedality, partially to well accommodated, as illustrated in figure 3b. These blocks had a coalesced microgranular substructure with weak pedality. The dominant porosity characterized in the thin section representative of the  $C\Delta\mu$  unit denotes an inferior microstructural quality when compared to the NAM unit, observing an increase in large planar pores (around 30 %) and small rounded and policoncave vughs (around 40 %), and a reduction in the compound packing pores (around 30 %). The change in the relative distribution of the  $C\Delta\mu$  unit when compared to the thin section of the NAM unit may be indicative of a compaction process by exhibiting a predominant porphyric relative distribution with aggregate coalescence and horizontal/sub-horizontal cracking.

The third MHU of this profile, designated as  $Fmt\Delta\mu$ , had an enaulic-porphyric relative distribution, subangular blocky structure and highly coalesced microgranular aggregates. There was a secondary enaulic area, restricted to vughs and channels with loose and continuous infillings. The porosity was dominated by rounded and policoncave vughs (55 %), followed by channels (20 %), and planar pores (25 %). In contrast to the previous  $C\Delta\mu$  unit, an increase in rounded and policoncave vughs and channels, together with a reduction in planar pores, was observed, indicating better quality in this fragmented microstructural unit (Table 1). Biological activity was more intense when compared to that observed in the  $C\Delta\mu$  unit and similar to the NAM unit, with widespread presence of biological galleries and vughs and channels.

The last MHU described in the profile of the Memory plot, and designated as  $Fpt\mu\Delta+tf$ , had an enaulic-porphyric relative distribution similar to the previous  $Fmt\Delta\mu$  unit, with a slightly denser microstructure in subangular blocks with moderately to strongly developed pedality, partially accommodated, and an intense process of cracking of the groundmass (Figure 3c). Secondarily, an area with the presence of a microgranular microstructure (enaulic) with a moderately developed pedality and partially accommodated aggregates was also observed, probably originating from the intense biological activity also observed in this unit.

The porosity in the dominant area of this unit ( $Fpt\mu\Delta+tf$ ) was of the fissure type with intense microfissuration within the primary subangular blocky aggregates (40 %), rounded and policoncave vughs (35 %), compound packing

**Table 1. Micromorphological characteristics of the morphologically homogeneous units (MHUs) of the soil profile of the Memory Plot**

	NAM	CΔμ	FmtΔμ	FptμΔ+tf
Groundmass	Coarse Material: 15 % Fine Material: 60-65 % Porosity: 25-30 %	Coarse Material: 15 % Fine Material: 65 % Porosity: 20 %	Coarse Material: 15 % Fine Material: 65 % Porosity: 20 %	Coarse Material: 15 % Fine Material: 65 % Porosity: 20 %
Relative distribution C/F <sup>(1)</sup>	Porphyric-Enaulic with some areas purely porphyric, and others enaulic.	Enaulic-porphyric with enaulic areas.	Enaulic-porphyric with enaulic areas.	Enaulic-porphyric with enaulic areas.
Coarse material	Polycrystalline quartz grains (100 %) with an average size ranging from 0.14 to 1.1 mm, sub-round and poorly selected blocks. Presence of iron nodules (5 %).	Polycrystalline quartz grains (100 %) with an average size ranging from 0.05 to 1.6 mm, sub-round and poorly selected blocks. Presence of iron nodules (5 %).	Polycrystalline quartz grains (100 %) with an average size ranging from 0.11 to 1.2 mm, sub-round and poorly selected blocks. Presence of iron nodules (5 %).	Polycrystalline quartz grains (100 %) with an average size ranging from 0.07 to 1.8 mm, sub-round and poorly selected blocks. Presence of iron nodules (5 %).
Fine material	Composition: clay and Fe oxides.	Composition: clay and Fe oxides.	Composition: clay and Fe oxides.	Composition: clay and Fe oxides.
Pores	Compound packing (50 %) and rounded and policoncave vughs (35 %), channels (5 %), and planar pores (10 %).	Compound packing (30 %) and rounded and small policoncave vughs (40 %), and large planar pores (30 %).	Rounded and policoncave vughs (55 %), planar pores (25 %), and channels (20 %).	Planar pores with intense cracking (40 %), rounded and policoncave vughs (40 %) and channels (20 %).
Microstructure	Complex microstructure: a predominant microgranular area with strongly to moderately developed pedality and partially accommodated aggregates. The other area is in subangular blocks with moderately developed pedality and partially accommodated aggregates.	Complex microstructure: a predominant area with subangular blocks with moderately developed pedality and partially to well accommodated aggregates, which has a coalesced microgranular substructure with weak pedality. The other area with microgranular microstructure with dominance of a moderately developed pedality and partially accommodated aggregates.	A predominant microstructure in subangular blocks with moderately developed pedality and partially accommodated aggregates, which has a coalesced microgranular substructure with weak pedality. The eunalic area is restricted to filled vughs.	A predominant microstructure in subangular blocks with moderately to strongly developed pedality and partially accommodated aggregates, which has a substructure in fissured subangular blocks. The eunalic area is restricted to filled vughs.
Pedofeatures	Textural: clay-iron coatings around the pores and aggregates (<5 %); infillings: loose and discontinuous formed by microaggregates of the groundmass, and dense continuous of clay with cross extinction. Amorphous: typical ferruginous nodules (10 %) with an average size of 0.29 mm. Excrements: presence of coprolites.	Textural: clay-iron coatings around the pores and aggregates (< 5 %); infillings: loose and discontinuous formed by microaggregates of the groundmass, and dense continuous of clay with cross extinction. Amorphous: typical ferruginous nodule (10 %) with an average size of 0.42 mm. Excrements: presence of coprolites.	Textural: clay-iron coatings around the pores and aggregates (< 5 %); infillings: loose and discontinuous formed by microaggregates of the groundmass, and dense continuous of clay with cross extinction. Amorphous: typical ferruginous nodule (10 %) with an average size of 0.36 mm. Excrements: presence of coprolites.	Textural: clay-iron coatings around the pores and aggregates (< 1 %); infillings: dense and discontinuous. Amorphous: typical ferruginous nodules (10 %) with an average size of 0.31 mm. Excrement: presence of coprolites.
Basic organic material	Debris fragments of roots in decomposition; Coprolites in the pores.	Debris fragments of roots in decomposition; Coprolites in the pores.	Debris fragments of roots in decomposition; Coprolites in the pores.	Many debris fragments of roots in decomposition; Coprolites in the pores.

<sup>(1)</sup> C/F: coarse material (C) and fine material (F) ratio. NAM: not altered by management; F or C: fragmented or continuous soil volume; Δμ or μΔ: compact or porous clods, with aggregates that are very compact (Δ), compact (Δμ) and in the process of compaction (μΔ); pt, mt, gt: small, medium, or large clods; and tf: fine soil.



**Table 2. Micromorphological characteristics of morphologically homogeneous units (MHUs) of the crop profile under the Conventional System (CS)**

	NAM	C $\Delta\mu$	C $\mu\Delta$	Fpt $\Delta\mu$	Fpt $\mu\Delta$ +tf
Groundmass	Coarse material: 10 % Fine material: 50-55 % Porosity: 35-40 %	Coarse material: 15 % Fine material: 65-70 % Porosity: 15-20 %	Coarse material: 15 % Fine material: 60 % Porosity: 20 %	Coarse material: 15 % Fine material: 65 % Porosity: 20 %	Coarse material: 10 % Fine material: 60-65 % Porosity: 25-30 %
Relative distribution C/F <sup>(1)</sup>	Enaulic with some porphyric-enausic areas	Enaulic-porphyric with aggregate coalescence and some enaulic areas.	Enaulic-porphyric with aggregate coalescence and some enaulic areas.	Same as C $\mu\Delta$ . However, 80 % of the thin section is porphyric.	Same as Fpt $\Delta\mu$ .
Coarse material	Polycrystalline quartz grains (100 %) with an average size ranging from 0.08 to 0.45 mm, sub-rounded and poorly selected blocks. Presence of iron nodules (5 %).	Polycrystalline quartz grains (100 %) with an average size ranging from 0.09 to 2.1 mm, sub-rounded and poorly selected blocks.	Same as C $\Delta\mu$ with an average size ranging from 0.06 to 1.12 mm.	Same as C $\mu\Delta$ with an average size ranging from 0.05 to 1.8 mm.	Same as Fpt $\Delta\mu$ with an average size ranging from 0.04 to 1.16 mm.
Fine material	Composition: clay and Fe oxides.	Same as NAM.	Same as NAM.	Same as NAM.	Same as NAM.
Pores	Compound packing (60 %), rounded and policoncave vughs (30 %), channels (5 %), and planar pores (5 %).	Compound packing (20 %), rounded and small policoncave vughs (35 %), planar pores (40 %), and channels (5 %).	Compound packing (10 %), rounded and large policoncave vughs (70 %), micropores (5 %).	Compound packing (10 %), rounded and policoncave vughs (50 %), large planar pores (20 %), and channels (20 %).	Large rounded and policoncave vughs (45 %), planar pores (25 %), channels (20 %), and compound packing pores (10 %).
Microstructure	Complex microstructure: a predominant area with microgranular structure, strongly to moderately developed pedality and partially accommodated aggregates. The other area has a subangular blocky structure with moderately developed pedality and partially accommodated aggregates.	Complex microstructure: a predominant area with a subangular blocky structure with weakly developed pedality and partially to well accommodated aggregates, which has a coalesced microgranular substructure with weak pedality.	A predominant microstructure in subangular blocks with weakly developed pedality and partially accommodated aggregates, which has a coalesced microgranular substructure with weak pedality.	A predominant microstructure in subangular blocks with weakly developed pedality and partially accommodated aggregates, which has a coalesced microgranular substructure with weak pedality.	Same as Fpt $\Delta\mu$ .
Pedofeatures	Textural: clay-iron coatings around the pores and aggregates (< 5 %); Infillings: loose and discontinuous formed by microaggregates of the groundmass, and dense continuous of clay with cross extinction. Amorphous: typical ferruginous nodules (10 %) with an average size of 0.39 mm. Excrements: presence of coprolites.	Textural: same as C $\Delta\mu$ . Amorphous: typical ferruginous nodules (10 %) with an average size of 0.78 mm. Excrements: presence of coprolites (> 2 %).	Textural: same as C $\Delta\mu$ . Amorphous: same as C $\Delta\mu$ but with an average size of 0.25 mm. Excrements: presence of coprolites. (> 2 %).	Textural: same as C $\Delta\mu$ but with absence of dense continuous infillings. Amorphous: same as C $\Delta\mu$ but with an average size of 0.18 mm. Excrements: coprolites.	Textural: same as C $\Delta\mu$ but with absence of dense continuous infillings; Amorphous: same as C $\Delta\mu$ but with an average size of 0.24 mm. Excrements: not observed.
Basic organic material	Debris fragments of roots in decomposition.	Debris fragments of roots in decomposition.	Absence of debris fragments of roots in decomposition.	Few debris fragments of roots in decomposition.	Few debris fragments of roots in decomposition.

<sup>(1)</sup> C/F: coarse material (C) and fine material (F) ratio. NAM: not altered by management; F or C: fragmented or continuous soil volume;  $\Delta\mu$  or  $\mu\Delta$ : compact or porous clods, with aggregates that are very compact ( $\Delta$ ), compact ( $\Delta\mu$ ) and in the process of compaction ( $\mu\Delta$ ); pt, mt, gt: small, medium, or large clods; and tf: fine soil.

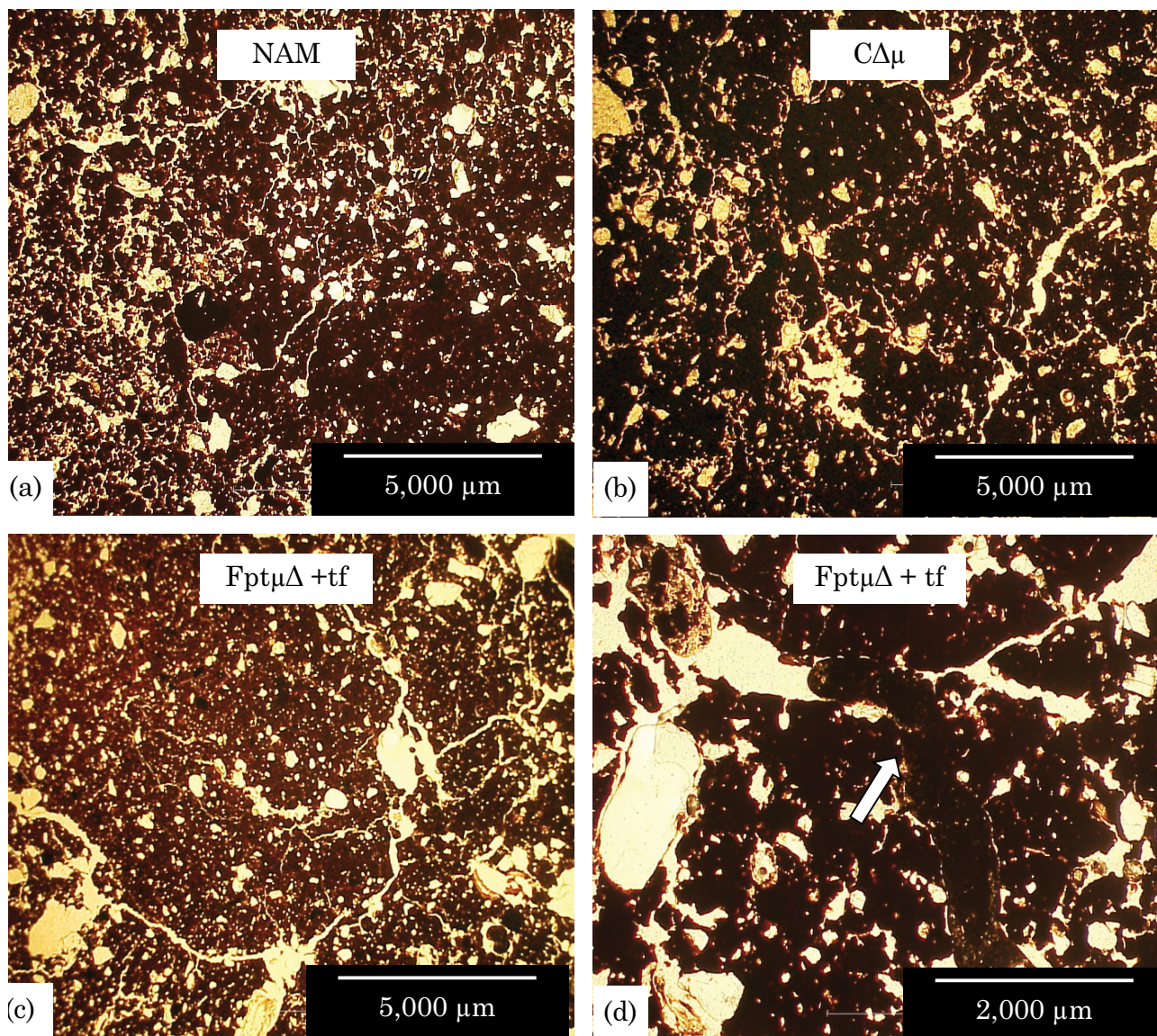


**Figure 3. Photomicrographs of the porosity predominant in different units described in the Memory plot: (a) porphyric-enaulic relative distribution; (b) porphyric relative distribution with coalescence of aggregates and horizontal cracking; (c) microstructure in subangular blocks with moderately to strongly developed pedality and partially accommodated aggregates; and (d) detail of excrement pedofeatures (coprolites). L: volume of loose soil, not compact, “powdered”; F or C: fragmented or continuous volumes of soil;  $\Delta\mu$  or  $\mu\Delta$ : compact or porous clods, with very compact aggregates ( $\Delta$ ), compact ( $\Delta\mu$ ) and in compaction process ( $\mu\Delta$ ); pt, mt, gt: small, medium or large clods; tf: fine soil; and NAM: not altered by management.**

(5 %), and channels (20 %). The microfissuration of the groundmass reflects the phenomena of soil expansion and contraction as a result of wetting and drying processes and root growth in the soil surface layers. Biological activity in this MHU was evidenced by the presence of vughs and channels of biological origin, and excremental features within the channels (coprolites) (Figure 3d). On the profile scale, the presence of white grubs, ants, and termites also showed the intense biological activity.

The presence of clay coatings, infillings and amorphous pedofeatures (ferruginous nodules), as well as fine and coarse fractions, are similar among the MHUs described in this plot, as noted in table 1.

Regarding soil micromorphology in CS (Table 2), the NAM unit had predominantly an enaulic relative distribution (very porous), with some porphyric-enaulic areas. The enaulic area had a microgranular microstructure, strongly to moderately developed pedality, and partially accommodated aggregates;

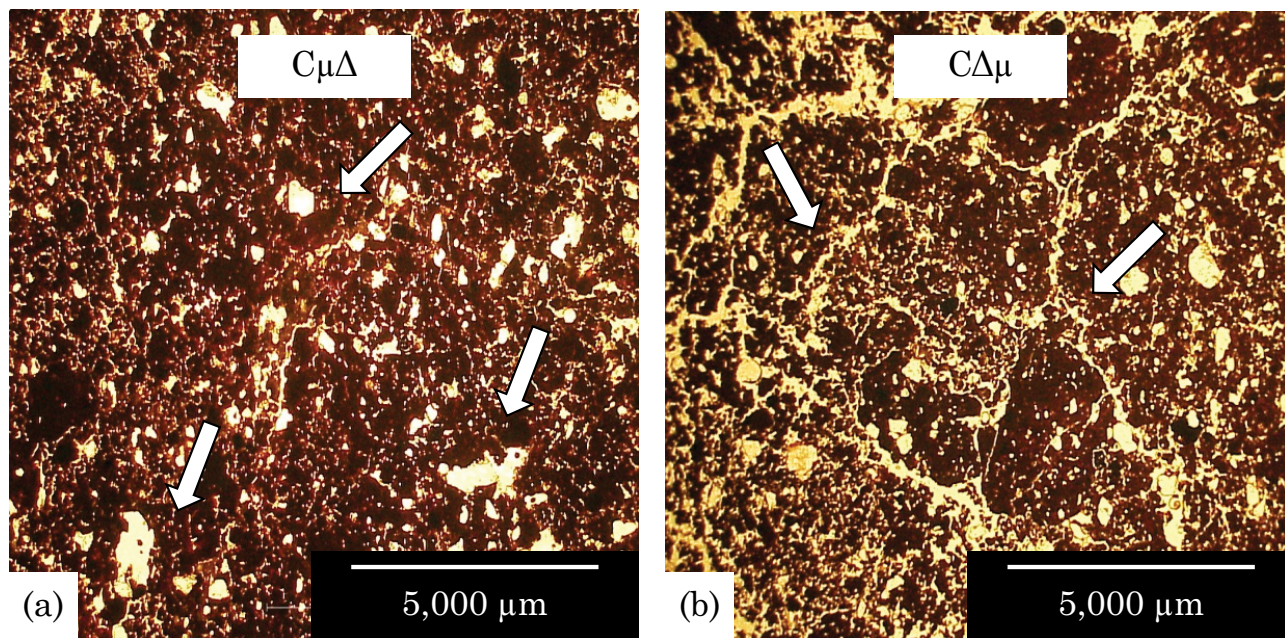


**Figure 4. Photomicrographs of the porosity predominant in  $C\mu\Delta$  and  $C\Delta\mu$  units described in the crop profile under CS: (a) rounded and large policoncave vughs, and (b) planar pores. C: continuous volumes of soil;  $\Delta\mu$  or  $\mu\Delta$ : compact or porous clods, with aggregates that are compact ( $\Delta\mu$ ) and in the process of compaction ( $\mu\Delta$ ).**

and in the porphyric-enauclic area, the microstructure was subangular blocky structure, with moderately developed pedality and partially accommodated aggregates. The predominance of microgranular microstructure in this MHU was also observed in the same unit in the Memory plot, which was expected since the structure of this volume was not altered by management and is typical of Oxisols. The dominant porosity of this unit was compound packing (60 %), followed by rounded and policoncave vughs (30 %), planar pores (5 %), and channels (5 %), similar to the distribution observed in the Memory plot profile. Biological activity in this unit was also evidenced by the presence of vughs and channels of biological origin, infilled or not, and by excrement features with the presence of coprolites in the channels.

The following two MHUs,  $C\mu\Delta$  and  $\Delta\mu$ , had composition of the groundmass, relative distribution, microstructure, and textural, amorphous, and excrement pedofeatures similar to each other, differentiated only by the types of predominating pores (Table 2).

In the  $C\mu\Delta$  unit, rounded and large policoncave vughs predominate (70 %), followed by microplanar pores (20 %) and compound packing (10 %), whereas in the  $C\Delta\mu$  unit, planar pores predominate (40 %), followed by rounded and policoncave vughs (35 %), compound packing pores (20 %), and channels (5 %) (Figures 4a,b). Such proportions and pores types with predominant planar pores and rounded and policoncave vughs in the  $C\Delta\mu$  unit indicated the

occurrence of physical force due to the intensive use of machinery in this management system, resulting in compaction.

Comparing the  $C\Delta\mu$  unit of the CS profile to the same unit of the Memory profile, changes in the microstructure and the proportion and types of pores were observed. Under CS, the aggregates had a greater degree of coalescence and an increase in planar pores, i.e., they were poorly developed, with a coalesced microgranular substructure with weakly developed pedality. These micromorphological observations of microstructure and porosity reinforced the observation of deterioration of the soil structure under CS in the subsurface compared to the Memory profile. These continuous units also showed signs of biological activity (coprolites) and decomposing roots fragments, though occurring to a lesser extent in relation to that observed under the Memory plot.

The fragmented units in the CS profile ( $Fpt\Delta\mu$  and  $Fpt\mu\Delta+tf$ ) were located near the surface and had a relative distribution similar to the  $C\Delta\mu$  type of MHU, but with a more coalesced microstructure and an increase in microplanar pores (Table 2). Aggregate coalescence and planar pores were also reported in fragmented units in the Memory plot when compared to the continuous units. The presence of planar pores and increased aggregate coalescence was interpreted as structural degradation. However, in terms of porosity, the fragmented units had greater porosity than the C units, as also observed

**Table 3. Descriptive statistics of the soil porosity data of the morphologically homogeneous units (MHUs) identified in the Memory Plot profile and Conventional System**

Plot	MHUs	N	Mean	s	Min.	Max.	CV
							%
Memory	NAM	13	27.36	3.43	19.69	32.48	12.55
	C $\Delta\mu$	14	18.18	4.98	11.41	28.52	27.42
	F $\mu\Delta\mu$	12	22.48	6.24	13.70	35.24	27.78
	F $\mu\Delta\mu$ +tf	11	18.27	5.55	10.45	28.11	30.38
Conventional system	NAM	11	33.91	4.42	26.91	40.8	13.03
	C $\mu\Delta$	15	21.00	6.35	13.37	35.83	30.26
	C $\Delta\mu$	14	13.58	6.41	5.82	29.73	47.24
	F $\mu\Delta\mu$	9	18.29	7.65	10.18	25.16	41.84
	F $\mu\Delta\mu$ +tf	11	18.55	5.81	10.44	28.11	31.30

N: number of replications; s: standard deviation; Min.: minimum; Max.: maximum; CV: coefficient of variation; NAM: not altered by management; F or C: fissure or continuous volume of soil;  $\Delta\mu$  or  $\mu\Delta$ : compact or porous clods, with aggregates that are very compact ( $\Delta$ ), compact ( $\Delta\mu$ ) and in the process of compaction ( $\mu\Delta$ ); pt, mt, gt: small, medium, or large clods; and tf: fine soil.

in the morphological evaluation of structure at the profile scale.

When comparing the degree of aggregate coalescence of the F $\mu\Delta\mu$ +tf unit of the CS profile and the Memory plot, we observed that in the latter the blocks had a moderately to strongly developed pedality but under CS weakly developed, reflecting worse structural quality. In this unit, few traces of biological activity were observed; however, debris fragments of decomposing roots were greater in number than those of the continuous units of the CS profile, and similar to the fragmented units of the Memory plot.

The results of descriptive analysis of soil porosity of the MHUs identified in the profiles of the Memory and CS plot are shown in table 3. According to the criteria defined by Warrick and Nielsen (1980), the data variability for the MHUs was average ( $12\% < CV < 60\%$ ). The highest values of the soil porosity coefficient of variation occurred in the units of the profile under CS, which is consistent with the fact that in this system a large number of mechanized operations translated into greater variability in the structural condition of the soil over short distances in the profile, which was reflected in porosity.

Results of statistical analysis of soil porosity characterized for the different MHUs of the Memory and CS plots showed that there were significant differences among units, as shown in figures 5 and 6.

In the Memory plot, the NAM unit showed the greatest porosity, differing significantly from the other MHUs (Figure 5). The average soil

porosity of the NAM unit of the Memory plot was 27.36 %, whereas that of the C $\Delta\mu$  unit was 18.18 %, which gives a reduction factor of 1.5. The average soil porosity values of the fragmented MHUs (F $\mu\Delta\mu$  and F $\mu\Delta\mu$ +tf) showed reduction factors of 1.21 and 1.49, respectively, compared to the unit not altered by management. These observations of porosity reduction corroborated with those given in the qualitative descriptions of the layers in micromorphological analyses, which reported a change from a porphyric-eunalic relative distribution to an eunalic-porphyric distribution.

Regarding the fragmented MHUs (F $\mu\Delta\mu$  and F $\mu\Delta\mu$ +tf), the means test indicated that they did not differ significantly among themselves or in relation to the soil porosity of the C $\Delta\mu$  unit at a 5 % of significance. Micromorphological descriptions also showed that these units have very similar porosities (Table 1), differing in the intensity of biological activity, with a higher proportion of channels in the fragmented units in relation to the continuous unit.

In the crop profile under SC, the average soil porosity of the NAM unit (33.91 %) was higher and differed from all other MHUs. The average soil porosity of the continuous unit C $\mu\Delta$  (21.0 %) was higher and differed from the average soil porosity of the continuous unit C $\Delta\mu$  (13.58 %). In the fragmented units F $\mu\Delta\mu$ +tf (18.55 %) and F $\mu\Delta\mu$  (18.29 %), the average soil porosities did not differ between themselves or in relation to the continuous units (Figure 6).

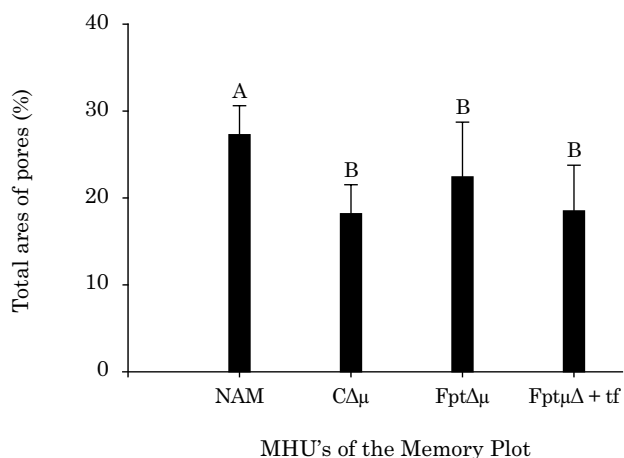


**Figure 5.** Results of the means test of soil porosity for MHUs of the Memory Plot profile. Means followed by the same uppercase letter do not differ regarding the MHUs, at 5 % of significance by Duncan's test. NAM: not altered by management; F or C: fragmented or continuous volumes of soil; Δμ or μΔ: compact or porous clods, with aggregates that are compact (Δμ) and in the process of compaction (μΔ); pt and mt: small and medium clods; and tf: fine soil.

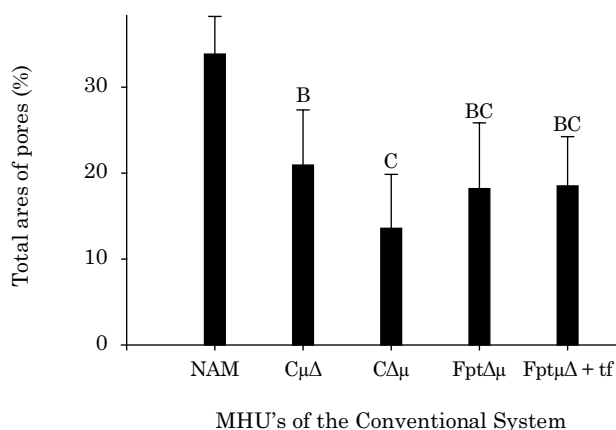


**Figure 6.** Results of the means test of soil porosity for MHUs of the crop profile under Conventional System (CS). Means followed by the same uppercase letter do not differ regarding the MHUs, at 5 % significance by Duncan's test. NAM: not altered by management; F or C: fragmented or continuous volumes of soil; Δμ or μΔ: compact or porous clods, with aggregates that are compact (Δμ) and in the process of compaction (μΔ); pt and mt: small and medium clods; and tf: fine soil.

The proximity of the mean soil porosity values of the continuous and fragmented MHUs in the crop profile under CS arose from the fact that they had the same microstructure, lower biological activity, and lower porosity in the form of vughs and channels.

Low porosity values reinforced the idea of structure deterioration in the subsurface of the soil under CS, reduction arising from the formation of a plow pan just below the cutting depth. Schaefer et al. (2001) found similar results in an Argissolo Vermelho-Amarelo [Typic Hapludult] tilled for 10 years with a heavy harrow, where analysis of polished blocks indicated an apparent decrease in macroporosity and an increase in soil compaction in the subsurface, shown by the presence of a plow pan and planar pores.

Analysis of the size and shape of the pores indicated significant changes in terms of percentage of the area in each one of the MHUs of the Memory (Figure 7) and CS (Figure 8) plots.

In both cases analyzed, most of the porosity found in the MHUs was in reference to complex pores, primarily of medium and large sizes. An exception to this was related to the CΔμ unit, which showed a predominance of medium to large size rounded pores in the Memory plot (Figure 7), and small to medium size rounded pores under CS (Figure 8). In general, all pore types were represented in all the profiles and MHUs described.

Figure 7 illustrates the relative distribution of the shapes (rounded, elongated, and complex) and sizes (small, medium, and large) of the MHU pores in the Memory plot profile. The pore distribution showed the predominance of complex pores in the NAM (15.03 %), FmtΔμ (11.72 %), and FptμΔ+tf (7.73 %) units compared to the CΔμ unit, where the predominance was of rounded pores (8.21 %). Regarding the proportion of elongated pores, the values were similar among MHUs, but with a slightly higher amount in fragmented MHUs.

The proportion of complex pores was highest in the NAM unit, followed by the FmtΔμ unit. The proportions of complex pores in the CΔμ and FptμΔ+tf units were similar and the lowest among the four MHU units. Thus, although these MHUs had similar porosities, as shown above, they differed in the type of predominant pores. In CΔμ, the higher proportion of rounded pores when compared to the FptμΔ+tf unit could be an indication that soil densing in CΔμ might have occurred by the transformation of compound packing (or complex) pores to mamelonar and policoncave (or rounded) vughs by microaggregate coalescence, as seen above in the micromorphological descriptions.

With respect to MHUs of the crop profile under CS, illustrated in figure 8, no distribution pattern

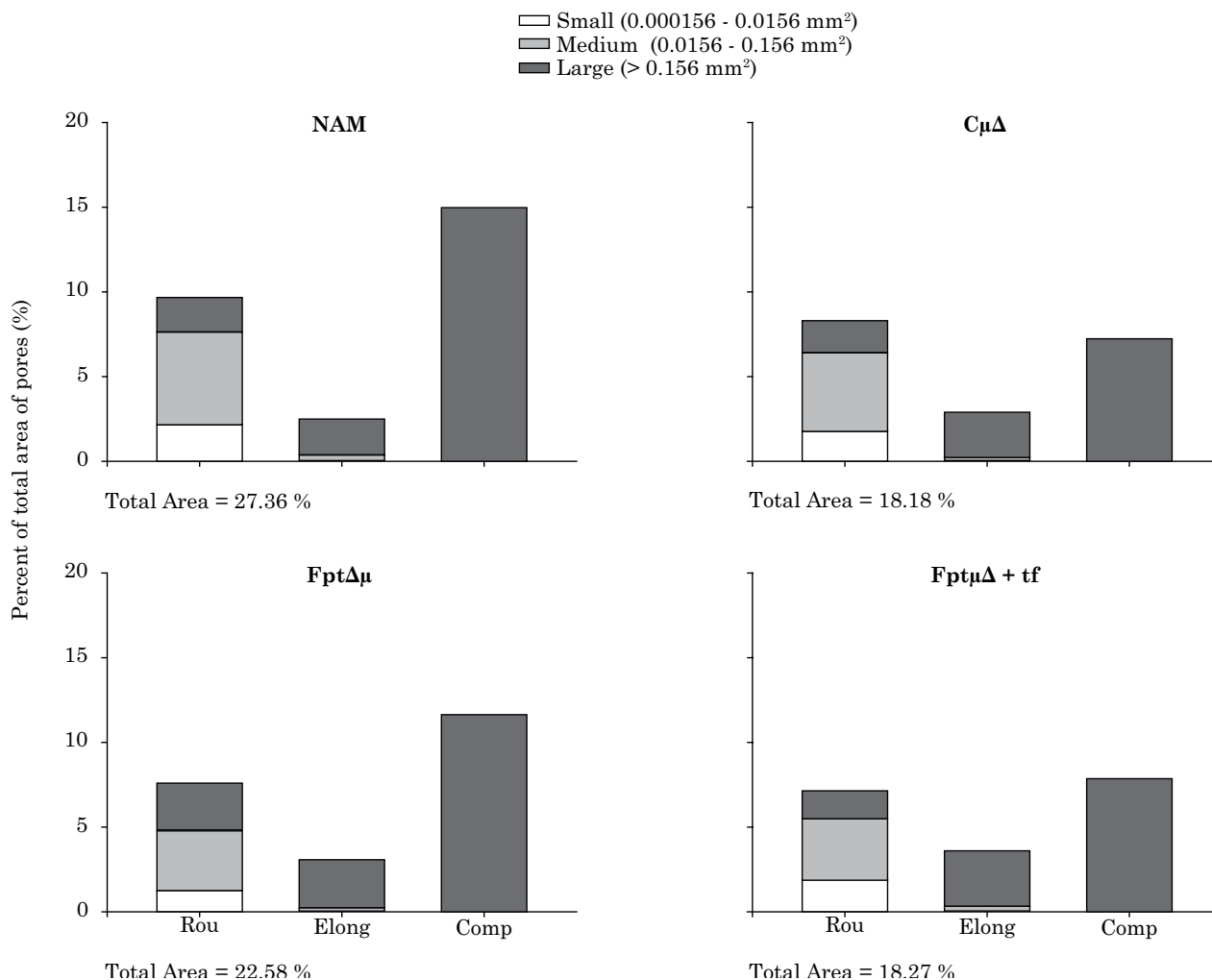


**Figure 7. Distribution of the total area of pores according to shape and size of the pores observed in the MHUs of the Memory plot. Rou: rounded; Elong: elongated; Comp: complex. NAM: not altered by management; F or C: fragmented or continuous volumes of soil;  $\Delta\mu$  or  $\mu\Delta$ : compact or porous clods, with aggregates that are very compact ( $\Delta$ ), compact ( $\Delta\mu$ ) and in the process of compaction ( $\mu\Delta$ ); pt, mt, gt: small, medium, or large clods; and tf: fine soil.**

of pore size and shape could be found, leading to a greater diversity of pores. This situation may reflect higher soil mobilization through the use of different implements for various agricultural operations, characteristic of conventional soil management systems, as shown by Tavares Filho and Tessier (2009).

Compared to the NAM unit, the C $\Delta\mu$  unit showed a decrease of approximately 40 % in soil porosity; this decrease is derived primarily from the reduction in complex pores. An increase in large and medium rounded pores and large elongated pores was seen, in this case associated with the planar pores observed in the qualitative description. The presence of these pores indicated compaction and degradation of the microstructure type.

Regarding the fragmented units (Fpt $\Delta\mu$  and Fpt $\mu\Delta$ +tf), an increase in elongated pores in comparison with the C $\Delta\mu$  unit was observed, corroborating the micromorphological descriptions that showed a more coalesced sub-microstructure with an increase in microplanar pores.

The drastic reduction in macro and mesopores in units C and F in this profile may be associated with soil compaction, which was also observed in the micromorphological descriptions. Pagliai et al. (1984) also reported the effect of agricultural machinery traffic on the soil, showing that after intensive traffic there was compaction in the subsoil, causing a reduction in total porosity, especially in the transmission pores (complex), to values that limited water movement and root growth.

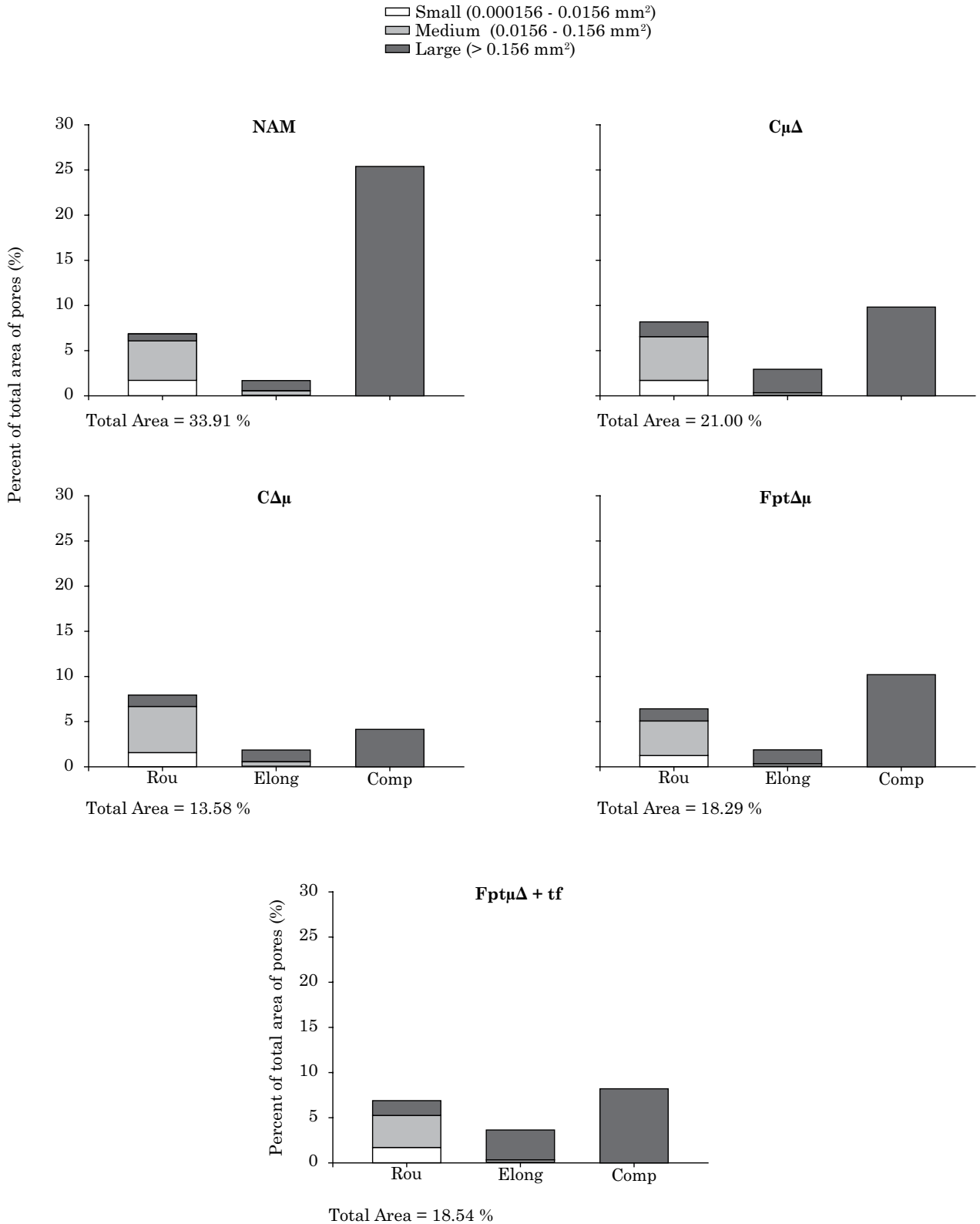


**Figure 8.** Distribution of the total area of pores according to shape and size of pores in the MHUs of the crop profile under Conventional System. Rou: rounded; Elong: elongated; Comp: complex. NAM: not altered by management; F or C: fragmented or continuous volumes of soil;  $\Delta\mu$  or  $\mu\Delta$ : compact or porous clods, with aggregates that are very compact ( $\Delta$ ), compact ( $\Delta\mu$ ) and in the process of compaction ( $\mu\Delta$ ); pt, mt, gt: small, medium, or large clods; and tf: fine soil.

Thus, higher soil porosity and a higher proportion of complex and elongated pores (channels) in the C MHUs of the Memory plot conferred a different arrangement to them and, hence, improved physical conditions for root penetration and soil water movement when compared to the C MHUs in CS. Observations on the crop profile scale showed a higher number of roots in the Memory plot when compared to CS.

## CONCLUSIONS

The MHUs under a Conventional Management System showed a matrix with a more compact relative distribution, and aggregate coalescence and microstructure in subangular blocks, which was different from the structure of the Memory plot units, which were more porous and showed granular microstructure.

Image analyses proved to be sensitive to the detection of changes in the morphology of the types of pores of the MHUs due to management. The predominance of compound packing pores and rounded vughs in the fragmented units of the Memory Plot characterize high biological and root activity.

## ACKNOWLEDGEMENTS

We thank the School of Agricultural Engineering at UNICAMP, the CNPq (National Council for Scientific and Technological Development) and the CAPES (Office for Improvement of Higher Education Personnel).

## REFERENCES

- Ball BC, Schjonning P. Air permeability. In: Dane JH, Topp C, editors. *Methods of soil analysis. Physical methods*. Madison: Soil Science Society of America; 2002. Part 4, p.1141-58.
- Bertol I, Albuquerque JA, Leite D, Amaral AJ, Zoldan Junior WA. Propriedades físicas do solo sob preparo convencional e semeadura direta em rotação e sucessão de culturas, comparadas às do campo nativo. *R Bras Ci Solo*. 2004;28:155-63.
- Bullock P, Fedoroff N, Jongerius A, Stoops G, Tursina T, Babel U. *Handbook for soil thin section description*. Albrington: Waine Reserch; 1985.
- Castro SS, Cooper M, Santos MC, Vidal-Torrado P. Micromorfologia do solo: Bases e aplicações. In: Curi N, Marques JJ, Guilherme LRG, Lima JM, Lopes AS, Alvarez V, VH, editores. *Tópicos em ciência do solo*. Viçosa, MG: Sociedade Brasileira de Ciência do Solo, 2003. v.3, p.107-64.
- Cooper M, Vidal-Torrado P, Grimaldi M. Soil structure transformations from ferralic to nitic horizons on a toposequence in southeastern Brazil. *R Bras Ci Solo*. 2010;34:1685-99.
- Curmi P, Kerttzman FF, Queiroz Neto JP. Degradation of structure and hydraulic properties in an Oxisol under cultivation (Brazil). In: Ringrose-Voase AJ, Humpherys GS, editors. *Soil micromorphology: Studies in management and genesis*. Amsterdam: Elsevier; 1994. p.569-579. (Developments in Soil Science, 22)
- Dersigny C, Guimarães MF, Visintin TMR. Observação do estado estrutural e da repartição espacial do sistema radicular do milho cultivado num Latossolo Roxo. In: *Anais do 8º Congresso Brasileiro e Encontro de Pesquisa sobre Conservação de Solo*; 1999; Londrina (PR). Londrina (PR): Sociedade Brasileira de Ciência do Solo; 1990. p.76.
- Dexter AR. Soil physical quality. Part I. Theory, effects of soil texture, density, organic matter, and effects on root growth. *Geoderma*. 2004;120:201-14.
- Drees LR, Karathanasis AD, Wilding LP, Blevins RL. Micromorphological characteristics of long-term no-till and conventionally tilled soils. *Soil Sci Soc Am J*. 1994;58:508-17.
- Doran JW. Microbial biomass and mineralizable nitrogen distributions in no tillage and plowed soils. *Biol Fertil Soil*. 1987;5:68-75.
- Empresa Brasileira de Pesquisa Agropecuária - Embrapa. *Sistema brasileiro de classificação de solos*. 3ª ed. Rio de Janeiro; 2013.
- Fregonezi GAF, Brossard M, Guimarães MF, Medina CC. Modificações morfológicas e físicas de um Latossolo argiloso sob pastagens. *R Bras Ci Solo*. 2001;25:1017-27.
- Gautronneau Y, Manichon H. *Guide méthodique du profil cultural*. Lyon: CEREF-Geara; 1987.
- Guimarães RML, Tormena CA, Alves SJ, Fidalski J, Blainski E. Tensile strength, friability and organic carbon in an Oxisol under a crop-livestock system. *Sci Agric*. 2009;66:499-505.
- Hakansson I, Voorhees WB, Riley H. Vehicle and wheel factors influencing soil compaction and crop response in different traffic regimes. *Soil Till Res*. 1988;11:239-82.
- Hallaire V, Cointepas JP. Caractérisation de la macroporosité d'un sol de verger par analyse d' image. *Agronomie*. 1993;13:155-164.
- Imhoff S, Silva AP, Tormena CA. Spatial heterogeneity of soil properties in areas under elephant-grass short duration grazing system. *Plant Soil*. 2000;219:161-8.
- Juhász CEP, Cooper M, Cursi PR, Ketzer AO, Toma, R.S. Savanna woodland soil micromorphology related to water retention. *Sci Agric*. 2007;64:344-54.
- Marques SR, Weill MAM, Silva LFS. Qualidade física de um Latossolo Vermelho, perdas por erosão e desenvolvimento do milho em dois sistemas de manejo. *Ci Agrotec*. 2010;34:967-74.
- Pagliai M, La Marca M, Lucamante G, Genovese L. Effects of zero and conventional tillage on the length and irregularity of elongated pores in a clay loam soil under viticulture. *Soil Till Res*. 1984;4:433-44.
- Reynolds WD, Drury CF, Yang XM, Tan CS. Optimal soil physical quality inferred through structural regression and parameter interactions. *Geoderma*. 2008;146:466-74.
- Santos RD, Lemos RC, Santos HD, Ker JC, Anjos LHC. *Manual de descrição e coleta de solo no campo*. 6ª ed. Viçosa, MG: Sociedade Brasileira da Ciência do Solo; 2013.



- Schaefer CER, Souza CM, Vallejos M, Viana JHM, Galvão JCC, Ribeiro LM. Características da porosidade de um Argissolo Vermelho-Amarelo submetido a diferentes sistemas de preparo de solo. *R Bras Ci Solo*. 2001;25:765-69.
- Shapiro SS, Wilk MB. An analysis of variance test for normality (complete samples). *Biometrika*. 1965;52:591-611.
- Silva AP, Kay BD, Perfect E. Characterization of the least limiting water range of soils. *Soil Sci Soc Am J*. 1994;8:1775-81.
- Soil Survey Division Staff. Soil survey manual. Washington: Soil Conservation Service of United States: 1993. (Handbook, 18)
- Souza ZM, Marques Júnior J, Cooper M, Pereira GT. Micromorfologia do solo e sua relação com atributos físicos e hídricos. *Pesq Agropec Bras*. 2006;41:487-92.
- Stoops G. Guidelines for analysis and description of soil and regolith thin sections. Madison: Soil Science Society of American; 2003.
- Tamia A, Moreau R, Fortier M, Yoro, G. Influence du travail du sol sur l'évolution physique d'un sol forestier ferrallitique après défrichement motorisé. *Étude Gestion Sols*. 1999;6:27-39.
- Tavares Filho J, Ralisch R, Guimarães MF, Medina CC, Balbino LC, Neves CSVJ. Método do perfil cultural para avaliação do estado físico de solos em condições tropicais. *R Bras Ci Solo*. 1999;23:393-9.
- Tavares Filho J, Tessier D. Characterization of soil structure and porosity under long-term conventional tillage and no-tillage systems. *R Bras Ci Solo*. 2009;33:1837-44.
- Thierfelder C, Wall PC. Rotation in conservation agriculture systems of Zambia: Effects on soil quality and water relations. *Exper Agric*. 2010;46:309-25.
- Xu X, Nieber JL, Gupta SC. Compaction effects on the gas diffusion coefficients in soil. *Soil Sci Soc Am J*. 1992;56:1743-50.
- Warrick AW, Nielsen DR. Spatial variability of soil physical properties in the field. In: Hillel D, editor. Applications of soil physics. New York: Academic Press; 1980. p.319-344.
- Weill MAM, Sparovek G. Estudo da erosão na microbacia do Ceveiro (Piracicaba, SP). II - Interpretação da tolerância de perda de solo utilizando a metodologia do índice de tempo de vida. *R Bras Ci Solo*. 2008;32:815-24.